Performance Modeling and Analysis of IEEE 802.11 IBSS PSM in Different Traffic Conditions

Pravati Swain, *Student Member, IEEE*, Sandip Chakraborty, *Student Member, IEEE*, Sukumar Nandi, *Senior Member, IEEE*, Purandar Bhaduri, *Member, IEEE*

Abstract—The IEEE 802.11 standard for wireless local area networks defines a power management algorithm for Independent Basic Service Set (IBSS) allowing it to save critical battery energy in low powered wireless devices. The power management algorithm for IBSS uses beacon intervals (BIs) as the time unit, where every BI consists of an Announcement Traffic Indication Message (ATIM) window and a data window. The stations that have data to send need to go through a handshaking procedure in the ATIM window. If this handshaking is successful, the station remains awake in the data window and participates in the data communication. Otherwise, it goes into the sleep mode. This paper presents an analytical model to compute the throughput, expected delay and expected power consumption in an IEEE 802.11 IBSS in Power Save Mode (PSM) for different traffic conditions in the network. The impact of data arrival rate, network size and size of the BI on the performance of the IEEE 802.11 DCF in PSM is also analyzed. This analysis reveals a clear trade-off among throughput, delay and average power consumption. The trade-off analysis is useful for designing efficient power consumption algorithms while maintaining the consistence performance of the network in terms of throughput and delay.

Index Terms—IEEE 802.11, IBSS, Power Save Mode, ATIM frame, Markov model, traffic analysis

1 Introduction

The IEEE 802.11 standard for Wireless Local Area Network (WLAN) medium access control and physical layer specification [1] supports two operating modes for wireless stations. The first one is *Infrastructure Basic Service Set*, where every wireless station communicates through an Access Point (AP) connected with the distribution system. The second communication mode is termed as Independent Basic Service Set (IBSS) where the stations create infrastructureless ad-hoc connections between themselves, and communicate with each other through a contention based channel access mechanism. IBSS has several applications ranging from mobile ad-hoc networks (MANETs) to vehicular and sensor networks. Several research directions are being explored to design effective channel access and routing mechanisms for utilizing the network resources effectively and efficiently. The wireless stations that form an IBSS are often battery enabled low power devices. Therefore, to save critical battery resources, the standard supports power save mode (PSM) operation along with the distributed coordination function (DCF) for MAC layer channel access. In PSM if a station does not send or receive data in a time slot then it should go into the sleep mode to save battery power that otherwise would be wasted due to the idle listening. To enable this design, the standard divides time into BIs, and every BI is divided into an ATIM window and a data window. The station that has data frames to send, is allowed to do so only if it can successfully transmit an ATIM frame in the ATIM window. A station that neither transmits nor receives an ATIM frame in the ATIM window goes into the sleep mode in the data window. There are several works that try to enhance the basic power save operations based on different network characterizations, such as [2] and the references therein. However, the basic algorithm remains similar to the standard with some amendments.

The authors are with the Department Computer Science and Engineering, Indian Institute of Technology, Guwahati, INDIA 781039. e-mail: {pravati, c.sandip, sukumar, pbhaduri}@iitg.ernet.in.

The performance of a network significantly depends on the traffic characteristics. In the context of network traffic analysis, the terms *'saturation'* and *'unsaturation'* have been used widely. These terminologies can be defined in two different contexts - based on (i) the data generation rate, and (ii) the network throughput. In the context of data generation rate, a station is called saturated if it transmits traffic at the maximum supported data rate, otherwise it is called unsaturated. In the context of network throughput, a network is called saturated, when the network throughput reaches its maximum value, otherwise it is called unsaturated. To avoid the ambiguity, the terms *'data saturation'* and *'data unsaturation'* are used to denote the traffic situation with respect to the data generation rate, and the terms *'network saturation'* and *'network unsaturation'* are used in the context of network throughput. It can be noted that network saturation does not indicate data saturation and vice versa. A network can be saturated with large number of stations, even when every individual station is not data saturated. Similarly, with a small number of data saturated stations, a network may still be in the unsaturated state.

Several researchers have modeled the IEEE 802.11 DCF channel access to characterize the contention based access mechanism [3]–[7]. However, all these works assume data saturation at individual stations. On the other hand, traffic in public wireless LANs follows self-similar characteristics [8], where data frames from users come in a burst. Therefore, only the stations that have frames to transmit contend for the channel access. Thus *data unsaturation* is common for practical wireless channel access scenarios. This paper analyzes network throughput, delay and power consumption for IEEE 802.11 DCF PSM considering different traffic conditions emphasizing both the data unsaturation and data saturation scenarios. The proposed analysis is based on a Markov Chain Model of IEEE 802.11 DCF PSM in the ATIM window along with the data window. The numerical values obtained from the proposed theoretical analysis are compared with the simulation results obtained from Qualnet 5.0.1 network simulator [9] to validate the proposed model. The effect of power saving on the network throughput and delay for different traffic conditions is analyzed for different network sizes and different BIs. This analysis reveals a clear trade-off among throughput, delay and average power consumptions. The trade-off analysis is useful for designing efficient power consumption algorithms while maintaining the consistent performance of the network in terms of throughput and delay.

2 Related Works

The modeling of IEEE 802.11 DCF based channel access has been pioneered by Bianchi [3] where the author has used a two dimensional Markov chain to model the binary exponential back-off (BEB) mechanism and showed the effect of contention window (CW) value on the network throughput. The analysis by Bianchi [3] considers both Carrier Sense Multiple Access with Collision Avoidance (CSMA/CA) based basic access mechanism and RTS/CTS access mechanism for virtual carrier sensing. Although the model provides a good approximation of the DCF performance, it considers an ideal channel condition and saturated network traffic scenario. Several works have extended Bianchi's analysis for IEEE 802.11 DCF. In [4], the authors have presented a three dimensional Markov chain model to analyze the IEEE 802.11 DCF in a heavy traffic load, in the absence of hidden terminals. They have shown the effect of retry limit and network size on the performance of MAC-layer channel access. Haitao *et al.* have analyzed the performance of a Reliable Transport Protocol (RTP) over the IEEE 802.11 DCF [5]. Several other works exist that consider constant CW [6], prioritized traffic [7] etc to model IEEE 802.11 channel access performance.

The works described till now do not consider channel conditions, and a traffic model with unsaturated data traffic scenario. In [10], the authors have presented an analytical model to account for burst frame arrival by adding an extra idle state after each frame transmission, where the number of idle states follow a geometric distribution. Yzheng *et al.* [11] have considered the impact of incoming traffic loads, different frame sizes, the MAC layer queue and the imperfect wireless channels on the performance of DCF protocol. In [12], the authors have modeled the DCF protocol in unsaturated heterogeneous conditions having different traffic arrival rates. They have considered fairness issues between competing flows. The paper [13] presented an analytical model of IEEE 802.11 in the presence of non ideal transmission channel and capture effects. Yi *et al.* [14] evaluated the hidden station effect on data unsaturation.

The effect of power saving on IEEE 802.11 DCF has not been addressed adequately by the existing analytical models. However, some works exist that have modeled the power consumption in IEEE 802.15.4 personal area networks. Nilsson *et al.* [15] have modeled the energy consumption at wireless interface for ad-hoc networks with contention based channel access. In [16], the authors have modeled the contention based MAC protocol for IEEE 802.15.4 network and analyzed the power consumption based on network traffic. In [17], the authors have presented an experimental analysis of the per frame energy consumption in IEEE 802.11 WLAN devices. In an earlier paper [18], we have presented the throughput, delay and power analysis of IEEE 802.11 DCF PSM in saturated traffic condition. However, the earlier model does not consider network and traffic unsaturation, and therefore does not reflect real world traffic scenarios. So, it is important to extend the analytical model [18] by considering data and network unsaturation at individual stations.

3 The IEEE 802.11 DCF in PSM

The IEEE 802.11 standard [1] uses DCF for MAC layer channel access. This paper considers the basic access mechanism for DCF. The DCF basic access combines the standard CSMA/CA protocol along with the BEB. Whenever a station has a data frame in its interface queue, it first senses the channel. If the medium is sensed idle for a period larger than the *Distributed Inter-frame Space* (DIFS) time then a station starts transmitting the data frame, otherwise it defers the transmission until the medium is free. The back-off time is chosen as follows;

$$\text{Back-off Time} = \text{Random()} \times \text{Slot Time}$$

where the random value is uniformly distributed between $[0, CW-1]$ where $CW_{\min} \le CW \le CW_{\max}$. $CW_{\min}$ and $CW_{\max}$ are the minimum and the maximum CW size. These values are based on the physical modulation characteristics. As long as the channel is sensed idle, the back-off counter is decremented. The back-off value is frozen when the channel is sensed busy. After each unsuccessful transmission, the value of CW is doubled up to $CW_{\max} = 2^m(CW_{\min})$. The constant m is called maximum back-off stage. For a successful transmission, the CW is reset to $CW_{\min}$.

The IEEE 802.11 standard [1] defines power save technique for IBSS. It is assumed that all the stations are synchronized, and are awake at the beginning of each BI. The stations in PSM wake up periodically to listen to the beacon messages, and stay awake for a period of time called the ATIM window. The ATIM frame is a control frame which is exchanged by the stations within the ATIM window to determine whether to go for PSM, or to stay awake for data transmission after the end of the ATIM window. When a station has a data frame to send, it first transmits an ATIM frame to the corresponding receiver during the ATIM window, following the 802.11 CSMA/CA DCF back-off mechanism as specified in the standard [1]. The IEEE 802.11 standard [1] does not define the retry limit for the ATIM frame transmission in IBSS. However, the paper [19] defines the retry limit of three for an ATIM frame transmission within an ATIM window and up to three BIs. If the ATIM frame is not transmitted successfully within an ATIM window, the corresponding data frame is buffered for the next beacon interval. After the third ATIM window, if the ATIM frame is not transmitted successfully then the data frame is dropped. A similar assumption is made in this paper to model the ATIM frame transmission.

After successful transmission of an ATIM frame, the ATIM sender and the receiver remain awake for the rest of the BI (data window) for data frame transmission, and the rest of the stations go into the sleep state to save battery energy. The data frame transmission is based on CSMA/CA along with the BEB. It can be noted that the standard does not specify the number of BIs for data frame transmission. In the paper [20] the authors have explained by theoretical analysis and simulation results that a single data window is sufficient to successfully transmit a data frame after transmitting an ATIM frame successfully in the ATIM window. A similar assumption is made in this paper for data frame transmission.

4 Modeling and Analysis of IEEE 802.11 PSM for Different Traffic Conditions

4.1 Network Model Assumption

The following assumptions are made to model and analyze the performance of IEEE 802.11 PSM at different traffic conditions.

1) The network consists of n stations with basic access mechanism enabled for data frame communication.
2) Every station has data traffic with probability α ($0 < \alpha \leq 1$), called the packet available probability. The value of α is derived from the frame generation rate at the application layer. If $\alpha = 1$, each station always has data frames to transmit (data saturation condition).
3) The retry limit for an ATIM frame is *three within one beacon interval*. [19]
4) A station can try at most *three beacon intervals* for successful transmission of one ATIM frame [19].
5) One data window is sufficient to successfully transmit a data frame, after transmitting an ATIM frame successfully in the ATIM window [20].
6) There is no higher layer buffering of data frames. When a data frame is generated, it is forwarded to the MAC layer. This point is assumed to isolate the higher layer effects over the MAC layer modeling.

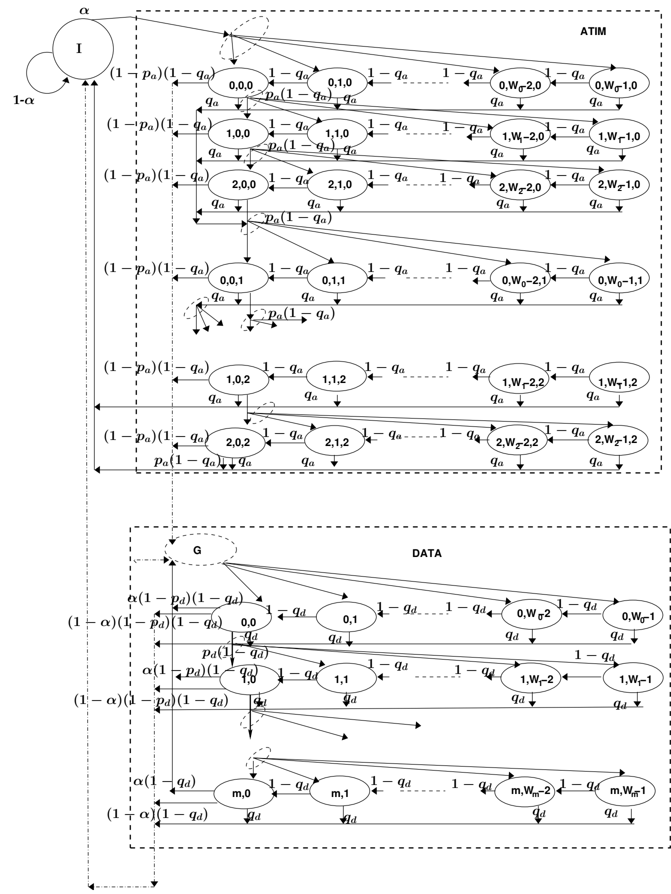

Fig. 1. Markov model for IEEE 802.11 IBSS PSM

4.2 System Model

Let the random process $s(t)$ represent the back-off stage, which denotes the retry limit to transmit an ATIM or a data frame within one BI. The second random process $b(t)$ is used to represent the back-off counter. Let the back-off counter be decremented by one at the beginning of each slot. The value of $b(t)$ depends on the back-off stage $s(t)$. In the i^{th} back-off stage ($s(t) = i$), the back-off counter value is within $[0, W_i - 1]$ where $W_i = 2^i W_0$ and W_0 is the initial CW ($CW_{\min}$). From the assumption in Subsection 4.1 (point 3), the value of the back-off stage $s(t)$ is within $\{0, 1, 2\}$ for the ATIM window. For the data window, $s(t)$ is within $\{0...m\}$, where m is the maximum retry limit to transmit a data frame in the data window. The third random process $a(t)$ represents the back-off layer that indicates the number of beacon intervals used to successfully transmit an ATIM frame. From the assumption in Subsection 4.1 (point 4), the value of the back-off layer $a(t)$ is within $\{0, 1, 2\}$.

The channel access mechanisms for the ATIM and the data frame transmissions in IEEE 802.11 IBSS PSM are modeled using two discrete time Markov models, one for the ATIM frame transmission and the other for the

$$
\begin{cases}
(1) \quad P\{I|I\} = 1-\alpha & \\
(2) \quad P\{(0,j,0)^{'}|I\} = \frac{\alpha}{W_0}, & j \in [0, W_0-1]; \\
(3) \quad P\{(i,j,k)^{'}|(i,j+1,k)^{'}\} = 1-q_a, & i \in [0,2], j \in [0, W_i-1], k \in [0,2]; \\
(4) \quad P\{(0,j,k+1)^{'}|(i,j',k)^{'}\} = \frac{q_a}{W_0}, & i \in [0,2], j \in [0, W_0-1], k \in [0,1], j' \in [0, W_i-1]; \\
(5) \quad P\{I|(i,j,2)^{'}\} = q_a, & i \in [0,2], j \in [0, W_i-1]; \\
(6) \quad P\{I|(2,0,2)^{'}\} = p_a \times (1-q_a), & \\
(7) \quad P\{(0,j,k+1)^{'}|(2,0,k)^{'}\} = \frac{p_a \times (1-q_a)}{W_0}, & j \in [0, W_0-1], k \in [0,1]; \\
(8) \quad P\{(i+1,j,k)^{'}|(i,0,k)^{'}\} = \frac{p_a \times (1-q_a)}{W_i}, & i \in [0,1], j \in [0, W_i-1], k \in [0,2]; \\
(9) \quad P\{(i,j)^{''}|(i,j+1)^{''}\} = 1-q_d, & i \in [0,m], j \in [0, W_i-1]; \\
(10) \quad P\{I|(i,j)^{''}\} = q_d, & i \in [0,m], j \in [0, W_i-1]; \\
(11) \quad P\{(0,j)^{''}|(i,0)^{''}\} = \frac{\alpha(1-p_d)(1-q_d)}{W_0}, & i \in [0,m], j \in [0, W_0-1]; \\
(12) \quad P\{I|(i,0)^{''}\} = (1-\alpha)(1-p_d)(1-q_d), & i \in [0,m]; \\
(13) \quad P\{(i+1,j)^{''}|(i,0)^{''}\} = \frac{p_d \times (1-q_d)}{W_i}, & i \in [0,m], j \in [0, W_i-1]; \\
(14) \quad P\{(0,j)^{''}|(m,0)^{''}\} = \frac{\alpha(1-q_d)}{W_0}, & j \in [0, W_0-1]; \\
(15) \quad P\{I|(m,0)^{''}\} = (1-\alpha)(1-q_d), &
\end{cases}
\tag{1}
$$

data frame transmission, as shown in Fig 1, where the state G is a dummy state to connect the two models as a representation of the combined procedure. As the two access mechanisms are independent, the inter-transitions between the two models are shown using dotted arrows. Although the two Markov models are independent, the number of active stations that participate in the channel access during the data window is governed by the probability of successful transmissions of the corresponding ATIM frames. Therefore, the number of active stations participating in the ATIM contention is determined by the data generation probability, whereas for the data window, the number of active stations participating in the contention depends on the data generation probability, as well as on the probability of successful transmissions in the ATIM window.

Another state I is introduced in the combined model to represent the data unsaturation at a station. State I caters to the following two situations:

- after a successful frame transmission, there is another frame in the buffer, with probability α,
- the buffer is empty, and the station waits for the next frame at state I with probability $1-\alpha$.

Let p_a denote the conditional collision probability in the ATIM window and p_d the same for the data window. The quantities q_a and q_d are the probabilities that the ATIM and data window end when a station is attempting to transmit an ATIM frame and a data frame respectively. The one-step non zero transition probabilities of the Markov chain in Fig. 1 are presented in equation (1), where a single prime ($'$) represents the transition probabilities in the ATIM window and a double prime ($''$) represents transition probabilities in the data window. These transition probabilities are summarized as follows;

1) The first equation represents the probability that the station has no frame in the buffer to transmit, $(1-\alpha)$.
2) The second equation states that a station has a data frame in the buffer to transmit with probability α.
3) The third equation indicates that within the ATIM window, the ATIM frame back-off counter decrements with probability $(1-q_a)$.
4) The fourth equation depicts that at any back-off stage and for any back-off counter value, if the ATIM window ends, the system tries to retransmit the ATIM frame with back-off stage 0 in the next ATIM window.
5) The fifth equation presents an unsuccessful transmission of an ATIM frame, when the ATIM window ends at the third BI (indicated by $a(t)=2$).
6) The sixth equation indicates that at the third ATIM window and at the last retry limit, the ATIM frame is discarded, and the buffer is checked for new data frame.
7) The seventh equation indicates that there is a collision at the last attempt within an ATIM window.
8) The eighth equation represents that the station increases the back-off stage, and selects the back-off counter uniformly after an unsuccessful transmission of an ATIM frame.
9) The ninth equation implies that within the data window the data frame back-off counter decrements with probability $(1-q_d)$.
10) The tenth equation indicates the end of data window has been reached at any back-off stage or any back-off counter, resulting in dropping of the data frame.
11) The eleventh equation models the successful transmission of a data frame, and the presence of has a next frame in the buffer to transmit with probability α.
12) The twelfth equation depicts that after a successful transmission of data frame the station goes to the idle state with probability $(1-\alpha)$.
13) The thirteenth equation represents that the station increases the back-off stage and chooses the back-off counter uniformly after an unsuccessful trans-

mission of a data frame within the data window.

14) The fourteenth equation models that there may be a successful or an unsuccessful transmission of a data frame at the last back-off stage, and the station has another frame in the buffer to be sent.
15) The fifteenth equation implies that at the last back-off stage, there may be a successful or an unsuccessful transmission of a data frame and the buffer is empty. So the station goes to the idle state.

4.3 Model Analysis

Let $b^{'}_{i,j,k}$ and $b^{''}_{i,j}$ be the stationary distributions of the Markov chain for the ATIM and the data windows, respectively. Here,

$$\begin{aligned} b^{'}_{i,j,k} &= \lim_{t\to\infty} P\{s(t)=i, b(t)=j, a(t)=k\}, \\ & \quad i\in[0,2], j\in[0,W_i-1], k\in[0,2] \end{aligned}$$

and

$$b^{''}_{i,j} = \lim_{t\to\infty} P\{s(t)=i, b(t)=j\}, i\in[0,m], j\in[0,W_i-1]$$

To obtain a closed-form solutions for the Markov chain presented in Fig. 1, iterative equation (2) and equation (3) are used:

$$b^{'}_{i,0,k} = \frac{p_a(1-q_a)}{W_i}\sum_{l=0}^{W_i-1}(1-q_a)^l b^{'}_{i-1,0,k} \quad 0<i\leq 2 \tag{2}$$

$$b^{''}_{i,0} = \frac{p_d(1-q_d)}{W_i}\sum_{l=0}^{W_i-1}(1-q_d)^l b^{''}_{i-1,0} \quad 0<i\leq m \tag{3}$$

The stationary probabilities for each state of the Markov models presented in Fig. 1 are derived in equation (4) and equation (5).

$$b^{'}_{i,j,k} = \begin{cases} \frac{\alpha}{W_0} b_I, & i=0, j=W_0-1, k=0; \\ M_1, & i=0, j\in[0,W_0-2], k=0; \\ M_2, & i=0, j=W_0-1, k\in[1,2] \end{cases} \tag{4}$$

$$b^{''}_{i,j} = \begin{cases} N_1, & i=0, j=W_0-1; \\ N_1\times N_2, & i=0, j\in[0,W_0-2] \end{cases} \tag{5}$$

The values of M_1, M_2, N_1 and N_2 are

$$\begin{aligned} M_1 &= \frac{\alpha}{W_0} b_I \times \sum_{l=0}^{W_0-(j+1)} (1-q_a)^l \\ M_2 &= \frac{1}{W_0}\left[p_a(1-q_a)b^{'}_{2,0,k-1} + q_a \sum_{i=0}^{2}\sum_{j=0}^{W_i-1} b^{'}_{i,j,k-1} \right] \\ N_1 &= \frac{P_{as}}{W_0}\Bigg[1+\alpha\Big((1-p_d)(1-q_d) \\ & \qquad \sum_{i=0}^{m-1} b^{''}_{i,0} + (1-q_d)b^{''}_{m,0}\Big)\Bigg] \\ N_2 &= \sum_{l=0}^{W_0-(j+1)} (1-q_d)^l \end{aligned}$$

Let P_{as} be the probability of successful transmission of an ATIM frame. The derivation of P_{as} is discussed later in the paper. The stationary probability in the state I is,

$$\begin{aligned} b_I &= b^{'}_{2,0,2} + q_a\sum_{j=1}^{W_2-1} b^{'}_{2,j,2} + \sum_{i=0}^{1}\sum_{j=0}^{W_i-1} b^{'}_{i,j,2} \\ & \qquad +(1-\alpha)b_I \\ &= \frac{1}{\alpha}\left[(1-q_a)b^{'}_{2,0,2} + q_a\sum_{i=0}^{2}\sum_{j=0}^{W_i-1} b^{'}_{i,j,2}\right] \end{aligned} \tag{6}$$

A normalization condition is required to compute the value of $b^{'}_{0,0,0}$. It can be noted that the normalization condition for the ATIM frame transmission is independent of the data frame model. The normalization equation is represented as,

$$1 = \sum_{k=0}^{2}\sum_{i=0}^{m}\sum_{j=0}^{W_i-1} b^{'}_{i,j,k} + b_I \tag{7}$$

From equation (2), equation (3), equation (6) and equation (7) the value of $b^{'}_{0,0,0}$ is written as,

$$b^{'}_{0,0,0} = \frac{1}{X(1+Y+Y^2L)} \tag{8}$$

where,

$$\begin{aligned} A &= \left(\frac{(1-q_a)p_a{}^2}{q_a}\right) \times \frac{1}{W_i} \times \left(1-(1-q_a)^{(W_i-j)}\right) \times \\ & \qquad \prod_{j=1}^{i-1}\left(\frac{1-(1-q_a)^{W_j}}{W_j}\right) \\ B &= \frac{((1-q_a)p_a)^2}{q_a}\prod_{j-1}^{2}\left(\frac{1-(1-q_a)^{W_j}}{W_j}\right) \\ C &= B\times p_a(1-q_a) \\ X &= \sum_{i=0}^{2}\sum_{j=0}^{W_i-1} A \\ Y &= \frac{1}{W_0}\left[C+q_aX\right]\sum_{l=0}^{W_0-1}(1-q_a)^l \\ L &= X + \frac{1}{\alpha}\left((1-q_a)B + q_aX\right) \end{aligned}$$

Let τ_a be the probability that a station transmits an ATIM frame in a randomly chosen slot. Hence,

$$\tau_a = \sum_{k=0}^{2}\sum_{i=0}^{2} b^{'}_{i,0,k} \tag{9}$$

The value of τ_a is obtained by solving equation (2), equation (4) and equation (8). The relation between p_a and τ_a is,

$$p_a = 1-(1-\tau_a)^{n'-1}. \tag{10}$$

where n' is the number of active stations participating in the contention at the ATIM window. As ATIM frames are generated instantaneously at the MAC layer in the ATIM window, if a station has a data frame to transmit n' can be approximated as, $n' = \lceil n\alpha \rceil$ where n is the total number of stations in a network. The values of τ_a and p_a are solved numerically using fixed point iteration. P_{as}

is the probability of successful transmission of an ATIM frame. P_{as} is calculated as follows:

$$P_{as} = \frac{n'\tau_a(1-\tau_a)^{(n'-1)}}{1-(1-\tau_a)^{n'}}. \quad (11)$$

Similarly, we find out the probability of success for a data frame transmission after successfully transmitting an ATIM frame. Let τ_d be the probability that a station transmits a data frame in a randomly chosen slot in the data window. So the value of τ_d depends on the value of τ_a. The τ_d is represented as:

$$\tau_d = \sum_{i=0}^{m} b''_{i,0} \quad (12)$$

From equation (3), the value of $b''_{i,0}$ is expressed in terms of $b''_{0,0}$ as follows:

$$\sum_{i=0}^{m} b''_{i,0} = \sum_{i=0}^{m} F_i b''_{0,0} \quad (13)$$

Where,

$$F_i = \left(\frac{p_d(1-q_d)}{q_d}\right)^i \prod_{j=1}^{i}\left(\frac{\{1-(1-q_d)^{W_j}\}}{W^j}\right)$$

Similarly, from equation (5), $b''_{0,0} = \frac{1}{R}$ where,

$$R = \frac{W_0 q_d}{\alpha(1-(1-q_d)^{W_0})} - \{(1-p_d)(1-q_d)\sum_{i=0}^{m-1} F_i + (1-q_d)F_m\} \quad (14)$$

The relation between p_d and τ_d is

$$p_d = 1-(1-\tau_d)^{(n''-1)}. \quad (15)$$

where n'' is the number of active stations participating in the contention at the data window. For simplicity, we assume that a sender can send multiple data frames only to a single receiver in a data window. Further according to assumption (6) as stated earlier, there is no higher layer buffering of data packets, and therefore n'' can be approximated as, $n'' = \lceil(n\alpha \times P_{as})\rceil$ where n is the total number of stations in the network. Let P_{tr} be the probability that there is at least one data frame transmission in the considered slot. Let P_{ds} be the joint probability that a data frame is transmitted successfully after the successful transmission of an ATIM frame. The values of P_{tr} and P_{ds} are given by,

$$P_{tr} = 1-(1-\tau_d)^{n''} \quad (16)$$

$$P_{ds} = \frac{n''\tau_d(1-\tau_d)^{n''-1}}{P_{tr}}. \quad (17)$$

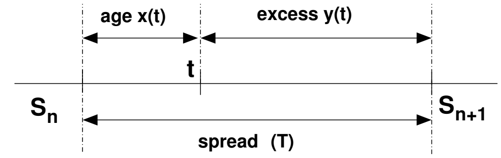

Fig. 2. The age and excess time of a renewal process [21]

4.4 Estimation of probability α, q_a, q_d

Let λ be the frame arrival rate at every station from the upper layer. Assuming the data traffic is generated according to a Poisson distribution[1], the probability α that a station has a data frame to send, is computed as;

$$\alpha = 1 - e^{-\lambda E[s_d]} \quad (18)$$

Here s_d is the duration of a data slot and $E[s_d]$ is the expected slot time in the data window. $E[s_d]$ is governed by the Markov model discussed earlier, and can be computed as follows. The average length of a slot in a data window is computed by considering three mutually exclusive and exhaustive cases. $(1-P_{tr})$ is the probability that a slot is empty, $P_{ds}P_{tr}$ is the probability of successful transmission of data, and $(1-P_{ds})P_{tr}$ is the collision probability for a data frame. Therefore,

$$E[s_d] = (1-P_{tr})\sigma + P_{ds}P_{tr}T_s + (1-P_{ds})P_{tr}T_c \quad (19)$$

Here T_s and T_c are the average time the channel is sensed busy because of a successful transmission or a collision in the data window, respectively and σ is the empty slot time. T_s and T_c are calculated as follows,

$$\begin{aligned} T_s &= \mathrm{DIFS} + H + E[P] + 2\delta + \mathrm{SIFS} + \mathrm{ACK} \\ T_c &= \mathrm{DIFS} + H + E[P] + \mathrm{SIFS} + \mathrm{ACK_{TO}} \end{aligned} \quad (20)$$

According to the assumption in Subsection 4.1 (point 1), every station accesses the channel using the basic access mechanism. Here DIFS and SIFS denote DCF inter-frame space time (in slots), and short interface space time (SIFS) respectively. ACK is the acknowledgment duration in slots. It has been assumed that all packets have the same size, so $E[P] = P$ is the average payload. The ACK timeout ($\mathrm{ACK_{TO}}$) is included in $\mathrm{T_c}$ according to the standard [1] specification, and a station waits for an EIFS time when the channel is sensed busy because of collision. Let $\mathrm{EIFS} = \mathrm{SIFS} + \mathrm{ACK_{TO}} + \mathrm{DIFS}$. $H = \mathrm{PHY_{hdr}} + \mathrm{MAC_{hdr}}$ be the packet header, and δ the propagation delay.

Let $Z(t)$ be a renewal process. The *spread* T of a renewal process is defined as the time interval after which the renewal occurs. The *age* of a renewal process $x(t)$ is defined as the time interval since the last renewal. The *excess* (or residual time) of a renewal process $y(t)$ is

1. The Poisson assumption of traffic generation is only a representative case used in this paper for modeling the effect of the traffic arrival on the MAC layer performance. Any other traffic distributions can be used depending on the specific scenarios, and the probability α, q_a and q_d can be calculated according to that distribution, following a similar procedure.

the time to the next renewal after t [21]. The spread, age and excess of a renewal process are shown in Fig. 2. Let S_i denote the time of the i^{th} renewal. It can be noted that $x(t)$ and $y(t)$ are independently distributed. As the traffic arrival is assumed to be Poisson, the time from t to the next renewal is exponentially distributed, and independent of all previously occurred renewals [22]. Therefore, $\{Z(t), t \geq 0, t \leq T\}$ is a Poisson process with rate λ. According to the theorem of *limiting distribution of excess time* [21],

$$P\{y(t) \leq s | t \leq T\} = \frac{1}{E[\kappa]} \sum_{i=0}^{s} P\{i \leq \kappa \leq T\} \tag{21}$$

where s is the minimum time duration to transmit an ATIM frame (in the ATIM window) or a data frame (in the data window), and κ is the inter-arrival time of the renewal process, such that $0 \leq \kappa \leq T$.

As discussed earlier, q_a and q_d denote the probability of the ending of the ATIM window and the data window respectively. The size of the ATIM window and data window is assumed to be fixed as mentioned in Section 4.1. The probabilities q_a and q_d depends on λ which is the packet arrival rate. That means they depend on network load. It is obvious that if the number of packets increase, the probability of q_a and q_d increase. Let $Z_a(t)$ denote the number of transmissions within an ATIM window, and $Z_d(t)$ the number of transmissions within a data window. Then $Z_a(t)$ and $Z_d(t)$ are two counting processes with inter-arrival time s_a and s_d respectively, where s_a and s_d are the durations of an generic ATIM slot and a generic data slot, respectively. The counting process of each state eventually reaches its steady state. Let $e_a(t)$ be the excess time in an ATIM window. In the ATIM window, every station waits for SIFS interval before accessing the channel. Then for an ATIM window, the probability of the ATIM window ending is expressed as the probability that excess time is less than the SIFS interval plus the mean slot duration in the ATIM window. Let T_{ATIM} be the size of the ATIM window. From equation (21),

$$\begin{aligned} q_a &= P(e_a(t) \leq \text{SIFS} + E[s_a] | t \leq T_{\text{ATIM}}) \\ &= \frac{1}{E[s_a]} \sum_{i=0}^{\text{SIFS}+E[s_a]} P\{i \leq s_a \leq T_{\text{ATIM}}\} \end{aligned} \tag{22}$$

where $E[s_a]$ is the expected slot duration in an ATIM window, calculated in a similar way as equation (19) using the success and failure probabilities of the ATIM window, the average channel busy time and the average collision time for an ATIM frame transmission. For a Poisson arrival at ATIM window, the value of $P\{i \leq s_a \leq T_{\text{ATIM}}\}$ can be obtained as follows;

$$\begin{aligned} & P\{i \leq s_a \leq T_{\text{ATIM}}\} \\ & \quad = \begin{cases} 1 & \text{when } i \leq \text{SIFS} \\ e^{-\lambda_a T_{\text{ATIM}}} - e^{-\lambda_a i} & \text{Otherwise} \end{cases} \end{aligned} \tag{23}$$

where λ_a is the ATIM frame arrival rate. The ATIM frame arrival rate is proportional to the data arrival rate, which depends on the number of active stations in the network. At the beginning of an ATIM window, ATIM frames are generated by the active stations in the network. Therefore, λ_a can be calculated as $n\alpha/T_{\text{ATIM}}$.

Similarly let $e_d(t)$ be the excess time for the data window. In a data window, every station waits for the DIFS interval for accessing the channel. Then for a data window, the probability that the data window ends is expressed as the probability that the excess time is less than the DIFS interval plus the mean slot duration in the data window. Let T_{DATA} be the size of the DATA window. So,

$$\begin{aligned} q_d &= P(e_d(t) \leq \text{DIFS} + E[s_d] | t \leq T_{\text{DATA}}) \\ &= \frac{1}{E[s_d]} \sum_{i=0}^{\text{DIFS}+E[s_d]} P\{i \leq s_d \leq T_{\text{DATA}}\} \end{aligned} \tag{24}$$

For a Poisson arrival at data window, the value of $P\{i \leq s_d \leq T_{\text{DATA}}\}$ can be obtained as follows;

$$\begin{aligned} & P\{i \leq s_d \leq T_{\text{DATA}}\} \\ & \quad = \begin{cases} 1 & \text{when } i \leq \text{DIFS} \\ e^{-\lambda T_{\text{DATA}}} - e^{-\lambda i} & \text{Otherwise} \end{cases} \end{aligned} \tag{25}$$

With the values of α, q_a and q_d in hand, the data window throughput and overall normalized throughput is derived, as presented in the next subsection.

4.5 Throughput Analysis

Let S_{DATA} denote the normalized system throughput in the data window for a network.

$$S_{\text{DATA}} = \frac{E[\text{payload information transmitted in a slot}]}{E[\text{duration of a slot}]}$$

Let, $E[P]$ be the average frame payload size (in terms of time unit, e.g., μs). Therefore,

$$S_{\text{DATA}} = \frac{P_{ds} P_{tr} E[P]}{E[s_d]} \tag{26}$$

S_{DATA} provides the channel throughput at the data window only and the value of $E[s_d]$ is presented in equation (19). The overall channel throughput has the ATIM overhead included with the data window throughput. The overall normalized throughput, S, is calculated as,

$$S = S_{\text{DATA}} \times \frac{\text{Data Window size}}{\text{Duration of BI}} \tag{27}$$

4.6 Average MAC Delay

The MAC layer channel access delay is an important parameter to analyze the performance of IEEE 802.11 IBSS. The average MAC delay is defined as the time between the arrival of a frame at the interface queue and the time it is delivered successfully. Let $\overline{D}$ denote the average MAC delay. Then $\overline{D}$ can be written as:

$$\overline{D} = \overline{D_{\text{succ}}^{(a)}} + \overline{D_{\text{succ}}^{(d)}} \tag{28}$$

where $\overline{D^{(a)}_{\text{succ}}}$ denotes the average delay in transmitting an ATIM frame successfully, and $\overline{D^{(d)}_{\text{succ}}}$ denotes the average delay in transmitting the corresponding data frame successfully.

Let $D^{(a)}_{\text{succ}}(k)$ be the delay experienced up to the k^{th} ATIM window to transmit an ATIM frame successfully. T_{ATIM} represents the fixed ATIM window size. Therefore,

$$D^{(a)}_{\text{succ}}(k) = k \times \mathrm{BI} + \mathrm{T}_{\text{ATIM}} \tag{29}$$

Assume that $D^{(d)}_{\text{succ}}(i,b)$ is the delay to transmit a data frame successfully in the i^{th} back-off stage of the data window. The sum of the back-off values up to stage i is b. Assume that b is the average value of the CW. Since $(W_i - 1)$ is the maximum CW size at the i^{th} back-off stage, the value of b is $\frac{Wi}{2}$. The value of $D^{(d)}_{\text{succ}}(i,b)$ is given by:

$$D^{(d)}_{\text{succ}}(i,b) = b \times T_{\text{avg}} + i \times T_c + T_s \tag{30}$$

Here T_s and T_c are the average time the channel is sensed busy because of a successful transmission or a collision, respectively, of the data frame in the data window.

Now, the average delay in transmitting an ATIM frame successfully is equal to the total delay upto the k^{th} ATIM window, given that the ATIM transmission success occurs at the k^{th} ATIM window. Let the probability $P^{(a)'}_{\text{succ}}(i,k)$ be the conditional probability that the back-off process of an ATIM frame transmission ends at the i^{th} stage of the k^{th} ATIM window, given that the ATIM frame is transmitted successfully. Then, the value of $\overline{D^{(a)}_{\text{succ}}}$ is calculated as:

$$\overline{D^{(a)}_{\text{succ}}} = \sum_{k=0}^{2}\sum_{i=0}^{2} P^{(a)'}_{\text{succ}}(i,k) \times D^{(a)}_{\text{succ}}(k) \tag{31}$$

Assume that $P^{(a)}_{\text{succ}}(i,k)$ is the probability that an ATIM frame is transmitted successfully at the i^{th} back-off stage of the k^{th} ATIM window, and $P^{(a)}_{\text{drop}}$ denotes the probability that an ATIM frame is dropped because of the retry limit being exceeded in the last ATIM window. $P^{(a)'}_{\text{succ}}(i,k)$ is calculated as follows:

$$P^{(a)'}_{\text{succ}}(i,k) = \frac{P^{(a)}_{\text{succ}}(i,k)}{1 - P^{(a)}_{\text{drop}}} \tag{32}$$

$P^{(a)}_{\text{succ}}(i,k)$ is given by:

$$P^{(a)}_{\text{succ}}(i,k) = X^i_k (1-p_a)(1-q_a) \tag{33}$$

where X^i_k is the probability that a station is unsuccessful in transmitting an ATIM frame till the $(i-1)^{th}$ back-off stage of the k^{th} ATIM window, and is given by:

$$X^i_k = \begin{cases} L^i, & k = 0; \\ L^{(3+i)} + q_a \times L^i, & k = 1; \\ L^{(3*2+i)} + 2 \times q_a \times L^{(3+i)} + q_a^2 \times L^i, & k = 2; \end{cases} \tag{34}$$

Here, $L = p_a(1-q_a)$. Consequently, $P^{(a)}_{\text{drop}}$ is calculated as:

$$P^{(a)}_{\text{drop}} = 1 - \sum_{k=0}^{2}\sum_{i=0}^{2} P^{(a)}_{\text{succ}}(i,k) \tag{35}$$

From equation (32) and equation (29), the average delay in transmitting an ATIM frame successfully ($\overline{D^{(a)}_{\text{succ}}}$) is calculated using equation (31).

The value of the average delay in transmitting a data frame successfully within the data window ($\overline{D^{(d)}_{\text{succ}}}$) is calculated in a similar way. Let $B(i)$ be the total back-off value up to i^{th} back-off stage, and $B(i)_{\max}$ be the summation of maximum contention window sizes up to the back-off stage i $\left(\sum_{j=0}^{i}(CW_j - 1)\right)$. Then, $\overline{D^{(d)}_{\text{succ}}}$ is calculated as:

$$\overline{D^{(d)}_{\text{succ}}} = \sum_{i=0}^{m}\sum_{b=0}^{B(i)_{\max}} P^{(d)'}_{\text{succ}}(i,b) \times D^{(d)}_{\text{succ}}(i,b). \tag{36}$$

The value $P^{(d)'}_{\text{succ}}(i,b)$ denotes the conditional probability that the back-off process of a data frame transmission ends at the i^{th} stage of the data window, with total back-off value b up to the i^{th} back-off stage, given that the data frame is transmitted successfully. $P^{(d)'}_{\text{succ}}(i,b)$ is given by:

$$P^{(d)'}_{\text{succ}}(i,b) = \frac{P^{(d)}_{\text{succ}}(i,b)}{1 - P^{(d)}_{\text{drop}}} \tag{37}$$

Here $P^{(d)}_{\text{drop}}$ is the probability of dropping a data frame that exceeds the retry limit in the data window. $P^{(d)}_{\text{succ}}(i,b)$ is the probability that a data frame is transmitted at the i^{th} stage and b is the sum of back-off values up to the i^{th} back-off stage. Therefore,

$$P^{d}_{\text{succ}}(i,b) = P^{(d)}_{\text{succ}}(i) Pr(B(i) = b)$$

$$P^{(d)}_{\text{drop}} = 1 - (1-p_d)(1-q_d)\sum_{i=0}^{m}\{p_d(1-q_d)\}^i$$

where m is the maximum retry limit to transmit a data frame in the data window. Assume, $P^{(d)}_{\text{succ}}(i)$ is the probability of transmitting a data frame successfully in the i^{th} back-off stage of the data window, and $p_d(1-q_d)$ is the probability that there is a collision within the data window. Therefore,

$$P^{(d)}_{\text{succ}}(i) = \{p_d(1-q_d)\}^i\{(1-p_d)(1-q_d)\} \tag{38}$$

Let $P^{(d)}_{\text{idle}}$, $P^{(d)}_{\text{col}}$ and $P^{(d)}_{\text{succ}}$ are the probability that a randomly chosen slot in the data window is idle, leads to a collision and results in successful transmission, respectively. Then,

$$\begin{aligned} P^{(d)}_{\text{idle}} &= (1-\tau_d) \\ P^{(d)}_{\text{succ}} &= n''\tau_d(1-\tau_d)^{(n''-1)} \\ P^{(d)}_{\text{col}} &= 1 - (1-\tau_d) - n''\tau_d(1-\tau_d)^{(n''-1)} \end{aligned}$$

Here τ_d, calculated according to equation (12), represents the probability that a station transmits a data frame in the randomly chosen slot in the data window and n'' is the number of station in active mode in the data window. Then,

$$T_{avg} = P^{(d)}_{\text{idle}}\sigma + P^{(d)}_{\text{succ}}T_s + P^{(d)}_{\text{col}}T_c \tag{39}$$

where σ is the empty slot time. From equation (37) and equation (30) the value of $\overline{D^{(d)}_{succ}}$ is calculated. Therefore, the average delay, calculated using equation (28), is given by:

$$\overline{D} = \sum_{k=0}^{2}\sum_{i=0}^{2}\left(P^{(a)'}_{\text{succ}}(i,k) \times D^{(a)}(k)\right) + \sum_{i=0}^{m}\sum_{b=0}^{B(j)_{max}}\left(P^{(d)'}_{\text{succ}}(i,b) \times D^{(d)}_{\text{succ}}(i,b)\right)$$

5 Average Power Consumption

In IEEE 802.11 IBSS PSM, the stations save critical battery power by going into the sleep mode whenever they do not have data to transmit as well as receive. Let PW_{tx}, PW_{rx}, PW_{idle} and PW_{sleep} denote the power consumed for data frame transmission, data frame reception, channel sensing and station in sleep mode respectively. $E[T_{\text{tx}}]$, $E[T_{\text{rx}}]$, $E[T_{\text{idle}}]$ and $E[T_{\text{sleep}}]$ are the expected time spent in transmit mode, receive mode, idle mode and sleep mode for per data frame transmission, respectively. The power consumed at a station can be classified into the following cases.

Transmit Power: If a station is a transmitter then the expected energy consumption in successful data frame transmission ($\overline{\xi_{tx}}$) is given by:

$$\overline{\xi_{tx}} = E[T_{\text{tx}}] \times PW_{tx} \tag{40}$$

$$E[T_{\text{tx}}] = \sum_{k=0}^{2}\sum_{i=0}^{2}\left(P^{(a)}_{\text{succ}}(i,k) \times (i \times T_{\text{acol}} + T_{\text{asucc}})\right) + \sum_{i=0}^{m}\left(P^{(d)}_{\text{succ}}(i) \times (i \times T_c + T_s)\right) \tag{41}$$

Let $P^{(a)}_{\text{succ}}(i,k)$ be the probability that an ATIM frame is transmitted successfully at the i^{th} back-off stage of the k^{th} ATIM window. Similarly, let $P^{(d)}_{\text{succ}}(i)$ denote the probability of transmitting a data frame successfully in the i^{th} back-off stage of the data window. The values of $P^{(a)}_{\text{succ}}(i,k)$ and $P^{(d)}_{\text{succ}}(i)$ are presented in equations (33) and equation (38) respectively.

T_{asucc} and T_{acol} are the average time for which the channel is sensed busy because of a successful transmission and a collision of an ATIM frame respectively. Therefore,

$$T_{\text{asucc}} = \text{ATIM}_{\text{framesize}} + \delta + \text{SIFS} + \text{ATIMACK}_{\text{TO}} + \delta$$
$$T_{\text{acol}} = \text{ATIM}_{\text{framesize}} + \text{SIFS} + \text{ATIMACK}_{\text{TO}}$$

Here $\text{ATIM}_{\text{framesize}}$ is the size of an ATIM frame in number of slots and $\text{ATIMACK}_{\text{TO}}$ is the timeout interval for ATIM acknowledgment. The value of T_c and T_s are presented in equation (20).

Receive Power: If a station does not have any data frame to transmit or has not successfully transmitted an ATIM frame, then there are two possibilities - if the station has successfully received an ATIM frame, then it acts as the receiver, otherwise it goes into sleep mode. Let the expected energy consumption in successful frame reception be $\overline{\xi_{rx}}$. Then,

$$\overline{\xi_{rx}} = E[T_{\text{rx}}] \times PW_{rx} \tag{42}$$

It can be noted that in an IBSS, the transceiver of station that is in the awake state, remains in the receive mode for the data or control frames that undergoes a collision. In those cases, the transceiver receives the signal, but decodes it as an invalid frame. On the other hand, all the stations which are going to receive a data frame in the DATA window, have to listen to all the ATIM frames in the ATIM phase. As on average $n\alpha$ stations transmit ATIM frames, therefore a station receives $n\alpha$ ATIM frames in the ATIM window, before it receives a data frame in the DATA window. So, the average receive time for a data frame is computed as;

$$E[T_{\text{rx}}] = \sum_{k=0}^{2}\sum_{i=0}^{2}\left(n\alpha P^{(a)}_{\text{succ}}(i,k) \times (i \times T_{\text{acol}} + T_{\text{asucc}})\right) + \sum_{i=0}^{m}\left(P^{(d)}_{\text{succ}}(i) \times (i \times T_c + T_s)\right) \tag{43}$$

Idle Power: A station remains in idle mode for two reasons;

1) The station is in the back-off stage, and so it remains idle for the back-off period.
2) The station has transmitted an ATIM frame successfully, and so it has to remain awake in the data window according to the standard. However it does not have sufficient data in its interface buffer, and it has transmitted all frames queued in its interface buffer before the data window ends. So, it has to remain in idle state either for the rest of the data window, or for the time before the next data arrives in its interface buffer, whichever is earlier.

Let the expected energy consumption in idle state be $\overline{\xi_{idle}}$. Then,

$$\overline{\xi_{\text{idle}}} = E[T_{\text{idle}}] \times PW_{idle} \tag{44}$$

Here,

$$E[T_{\text{idle}}] = E[T^{a}_{\text{idle}}] + E[T^{d}_{\text{idle}}] \tag{45}$$

According to the standard, if a station transmits one ATIM frame successfully, then it cannot send another ATIM frame in the same ATIM window. However, the station has to remain awake for the entire ATIM window. Thus the idle time in ATIM window has two components - expected idle time during back-off period at the ATIM window ($E[T^a_{\text{back-off}}]$) and expected idle time after transmitting one ATIM frame successfully, for the rest of the ATIM interval ($E[T^a_{\text{idle}_{\text{nd}}}]$). Thus,

$$E[T^a_{\text{idle}}] = E[T^a_{\text{back-off}}] + E[T^a_{\text{idle}_{\text{nd}}}] \tag{46}$$

$E[T^a_{\text{back-off}}]$ is given by:

$$E[T^a_{\text{back-off}}] = \sum_{k=0}^{2}\sum_{i=0}^{2}\left(P^{(a)}_{\text{succ}}(i,k)\times\left(\frac{W_i}{2}\times\sigma\right)\right)$$

In an IBSS, the transceiver of an station that is in awake state, remains idle only when it neither transmits nor receives a packet. Further, the transceiver remains in the receive state for all the ongoing communication in the network, may it be intended for that station or an overheard communication. In the ATIM window, on average $n\alpha$ stations transmit ATIM frames, and therefore every station receives $n\alpha$ ATIM frames on average. Consequently, $E[T^a_{\text{idle}_{\text{nd}}}]$ is computed as,

$$\begin{aligned}E[T^a_{\text{idle}_{\text{nd}}}] = &\sum_{k=0}^{2}\sum_{i=0}^{2}\Big(P^{(a)}_{\text{succ}}(i,k)\times \\ &(\mathrm{T}_{\text{ATIM}} - (i\times T_{\text{acol}} + (1+n\alpha)T_{\text{asucc}}))\Big)\end{aligned}$$

In the above equation, the quantity $(1+n\alpha)T_{\text{asucc}}$ denotes the time for one ATIM frame transmission and $n\alpha$ numbers of ATIM frames receptions. As mentioned earlier, T_{ATIM} represents the time duration of an ATIM window and σ is the duration of one slot time.

For the data window, the idle time is calculated as,

$$E[T^d_{\text{idle}}] = E[T^d_{\text{back-off}}] + E[T^d_{\text{idle}_{\text{nd}}}] \tag{47}$$

where $E[T^d_{\text{back-off}}]$ denotes the expected idle time in back-off period in data window and $E[T^d_{\text{idle}_{\text{nd}}}]$ denotes the expected idle time. $E[T^d_{\text{back-off}}]$ is given by:

$$E[T^d_{\text{back-off}}] = \sum_{i=0}^{m} P^{(d)}_{\text{succ}}(i)\times\left(\frac{W_i}{2}\times\sigma\right)$$

In the DATA window, a station remains in the idle state after a successful transmission if all of these conditions hold;

(i) *The station is not a transmitter*: This indicates that the station does not have any data to transmit. The probability for this is $(1-\alpha)$.

(ii) *The station is not a receiver*: In the DATA window, a station is not a receiver, when neither of the $n\alpha\times P_{\text{as}}$ stations, that are in the awake state, have a data frame to transmit. The probability of this event is $(1-\alpha)^{n\alpha\times P_{\text{as}}}$.

Therefore, after a successful data transmission, the average idle time is computed as

$$\begin{aligned}E[T^d_{\text{idle}_{\text{nd}}}] &= (1-\alpha)(1-\alpha)^{n\alpha\times P_{\text{as}}}\times T_{\text{DATA}} \\ &= (1-\alpha)^{(1+n\alpha\times P_{\text{as}})}\times T_{\text{DATA}}\end{aligned}$$

Here T_{DATA} represents the time duration of an data window.

Sleep Power: A station can go into the sleep mode if it neither transmits nor receives an ATIM frame in the ATIM window. Let $\overline{\xi_{sleep}}$ be the expected energy consumption during sleep mode. Then,

$$\overline{\xi_{sleep}} = E[T_{\text{sleep}}]\times PW_{sleep} \tag{48}$$

where $E[T_{\text{sleep}}]$ is the expected time duration of the sleep mode, which is given by:

$$\begin{aligned}E[T_{\text{sleep}}] = &\sum_{k=0}^{2}\left(1-\sum_{i=0}^{2}P^{(a)}_{\text{succ}}(i,k)\right)\times k \\ &\times\left(1-\frac{P_{as}}{n'}\right)\times T_{DATA}\end{aligned} \tag{49}$$

Here P_{as} is the probability of successful transmission of ATIM frame.

Let $\overline{PW}$ be the average power consumed by a station. Therefore,

$$\overline{PW} = \frac{\overline{\xi_{\text{tx}}}+\overline{\xi_{\text{rx}}}+\overline{\xi_{\text{idle}}}+\overline{\xi_{\text{sleep}}}}{E[T_{\text{tx}}]+E[T_{\text{rx}}]+E[T_{\text{idle}}]+E[T_{\text{sleep}}]} \tag{50}$$

$\overline{PW}$ shows the average power consumption by all the stations in a network. However, it does not reflect the distribution of power consumption among the stations. To analyze the power distribution among the stations, the standard deviation of power consumption is required along with the average power consumption which is presented in the next subsection.

5.1 Standard Deviation of Power Consumption

The standard deviation is the square root of variance. Assume that V is the variance in energy consumption and $\mathbb{H}$ is the variance in power consumption. V_{tx}, V_{rx}, V_{idle}, V_{sleep} are variances of energy consumption in transmit mode, receive mode, idle mode and sleep mode respectively. Therefore,

$$V = V_{\text{tx}} + V_{\text{rx}} + V_{\text{idle}} + V_{\text{sleep}} \tag{51}$$

Further the average power consumption per transmission is the ratio of the average energy consumed per transmission to the expected time of a transmission. As the expected time of a transmission is independent of the average energy consumed per transmission (it can be noted that the reverse is not true), therefore, the variance in power consumption per transmission can be expressed as the ratio of the variance in energy consumed per transmission to the average duration of a transmission. Therefore,

$$\mathbb{H} = \frac{V_{\text{tx}}+V_{\text{rx}}+V_{\text{idle}}+V_{\text{sleep}}}{E[T_{\text{tx}}]+E[T_{\text{rx}}]+E[T_{\text{idle}}]+E[T_{\text{sleep}}]} \tag{52}$$

$E[T_{\text{tx}}]$, $E[T_{\text{rx}}]$, $E[T_{\text{idle}}]$ and $E[T_{\text{sleep}}]$ are the expected time spent in transmit mode, receive mode, idle mode and sleep mode respectively. The value of $E[T_{\text{tx}}]$, $E[T_{\text{rx}}]$, $E[T_{\text{idle}}]$ and $E[T_{\text{sleep}}]$ are presented in equation (41), equation (43), equation (45) and equation (49) respectively. V_{tx}, V_{rx}, V_{idle}, and V_{sleep} are computed as follows.

- The variance of energy consumption in transmit mode ($V_{\rm tx}$) is expressed as;

$$V_{\rm tx} = E[T_{\rm tx}^2] \times PW_{tx} - \left(\overline{\xi_{tx}}\right)^2 \tag{53}$$

Here, $T_{\rm tx}$ represents the time spent in transmit mode. The value of $E[T_{\rm tx}^2]$ is calculated using an approach similar to equation (41). The quantity $\overline{\xi_{tx}}$ is the expected energy consumption in successful frame transmission.

- The variance of energy consumption in receive mode ($V_{\rm rx}$) is given by:

$$V_{\rm rx} = E[T_{\rm rx}^2] \times PW_{rx} - \left(\overline{\xi_{rx}}\right)^2 \tag{54}$$

Here, $E[T_{\rm rx}^2]$ is calculated using using an approach similar to equation (43). The quantity $\overline{\xi_{rx}}$ is the expected energy consumption in successful frame reception.

- The variance of energy consumption in idle mode ($V_{\rm idle}$) is expressed as;

$$V_{\rm idle} = E[T_{\rm idle}^2] \times PW_{\rm idle} - \left(\overline{\xi_{\rm idle}}\right)^2 \tag{55}$$

Here, $E[T_{\rm idle}^2]$ is calculated using using an approach similar to equation (45). The quantity $\overline{\xi_{rx}}$ is the expected energy consumption in idle state.

- The variance of energy consumption in sleep mode ($V_{\rm sleep}$) is given by:

$$V_{\rm sleep} = E[T_{\rm sleep}^2] \times PW_{\rm sleep} - \left(\overline{\xi_{\rm sleep}}\right)^2 \tag{56}$$

Here, $E[T_{\rm sleep}^2]$ is calculated using using an approach similar to equation (49). The quantity $\overline{\xi_{rx}}$ is the expected energy consumption during sleep mode.

6 Model Validation and Performance Evaluation

The proposed analytical model has been validated using the network simulator Qualnet 5.0.1 [9]. The system parameters are listed in Table 1. $CW_{\min}$ is the minimum CW, $CW_{\max}^a$ and $CW_{\max}^d$ are maximum CW for the ATIM and the data window respectively. The power consumption in different states are taken from the datasheet of Cisco Aironet 350 Series Client Adapters [23]. In simulation, the size of the ATIM window is taken to be $20ms$ for IBSS PSM. The simulation is executed for 10 different cases with randomly generated seed values, and the average values are plotted. Every individual simulation test case is executed for 200 seconds. In the simulation scenario, every station has an interface size of 1024 Kbytes, the transceiver uses transmit power of 15 dBm, with a receive sensitivity of -87 dBm. The antenna gain is considered to be 15 dB with 10 dB noise factor. For the simulation purpose, we have considered a time-variant channel with statistical propagation model, with two-ray path-loss and constant shadowing model. The shadowing mean and the correlation factor are considered to be 4.0 and 0.5, respectively. The stations are considered to be static.

TABLE 1
Parameters used in the simulation

Parameter	value	Parameter	value
Payload size	1024 bytes	PHY header	192μs
ACK	14 bytes + PHY header	ATIM	28 bytes + PHY header
MAC header	28 bytes	Basic rate	1Mbps
Data rate	2Mbps	Slot time	20μs
SIFS	10μs	DIFS	50μs
$CW_{\min}$	32	$CW_{\max}^a$	128
$CW_{\max}^d$	1024	$PW_{\rm tx/rx}$	2.25W (Watt)
$PW_{\rm idle}$	1.35W (Watt)	$PW_{\rm sleep}$	0.07W (Watt)

Fig. 3 presents the normalized throughput against different arrival rates having a fixed network with $n = 20$ and BI = $200ms$ (with fixed ATIM window at 20 ms). The figure shows that there is a good agreement between the two. However, there is a marginal gap between the theoretical and simulation results, as the theoretical model assumes a time-invariant channel without any channel loss, shadowing and path loss. The comparison between the theoretical and the simulation results shows that, although the proposed model approximates the performance by considering an ideal channel without any channel loss or propagation effect, the actual throughput performance, as observed from the simulation, deviates marginally from the predictive results obtained from the proposed model. Further both the theoretical and the simulation results follow similar pattern, and therefore the proposed theoretical model can be used for predictive and comparison purposes.

For different traffic generation rates, Fig. 4 and Fig. 5 (results obtained from analytical model) show how the normalized throughput depends on network size and the size of the BI. The observations from Fig. 3, Fig. 4 and Fig. 5 are summarized as follows.

- The throughput increases rapidly when the data arrival rate varies from 1 frames/second to 10 frames/second. After 10 frames/seconds, the network becomes saturated[2]. For frame arrival rate 10 frames/second to 40 frames/second, the throughput decreases slowly. During this period, the network throughput decreases because of the increasing contention among stations in the saturated network.
- The network throughput stabilizes when the data arrival rate is more than 40 frames/second. Normalized throughput remains almost fixed when the data arrival rate is beyond 40 frames/second (network size $n = 20$).
- It can be seen from Fig. 4 that as the size of the BI increases with a fixed ATIM window at 20 ms, the normalized network throughput increases. For a fixed ATIM window size at 20 ms, the size of the data window increases with the increase of the

2. It can be noted that data saturation at every individual station occurs at 100 frames/second.

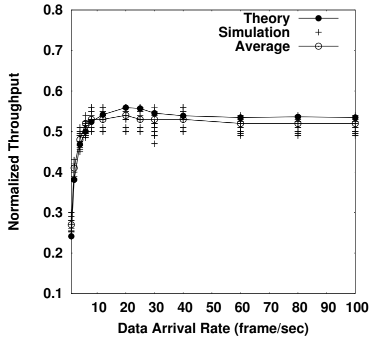

Fig. 3. Throughput for $n = 20$

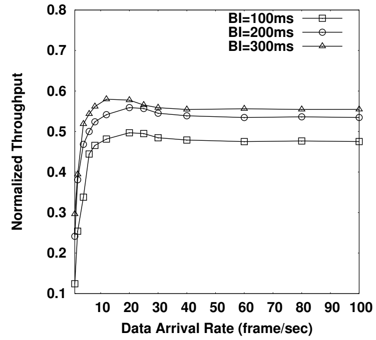

Fig. 4. Throughput for $n = 20$

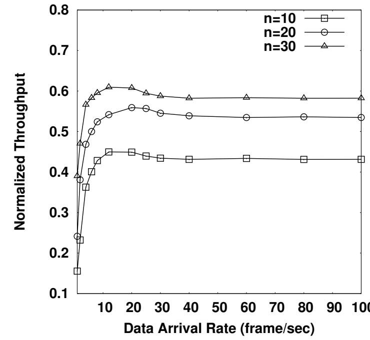

Fig. 5. Throughput for $BI = 200ms$

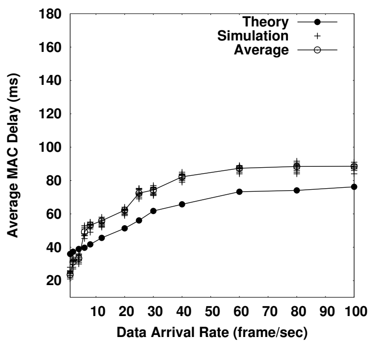

Fig. 6. Delay for $n = 20$

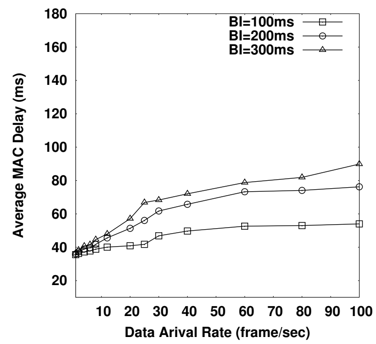

Fig. 7. Delay for $n = 20$

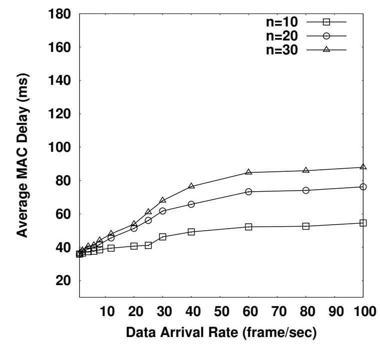

Fig. 8. Delay for $BI = 200$

BI. Thus the ATIM overhead becomes low which increases the overall network throughput.

- Fig. 5 shows the effect of the number of stations over the network throughput for fixed BI size at 200 ms. The ATIM window size is also fixed at 20 ms. As the number of stations increases, the overall throughput at network saturation also increases. After network saturation, the network throughput tends to decrease. When the network is highly loaded (data arrival rate is greater that 20 packets per second), the network throughput decreases because of the increased contention. Increasing the number of stations after network saturation increases the contention for channel access that results in marginally lower throughput.

Fig. 6 shows the average MAC delay against the frame arrival rate. Though both the curves follow similar trends, there is a slight gap between the theoretical and the simulation results. The difference between the two is because of the ideal channel assumption in our model, as discussed earlier. The numerical results from the analytical model are presented in Fig. 7 and Fig. 8. Fig. 7 presents the impact of the BI size (with fixed ATIM window at 20 ms) on the average MAC delay for different frame arrival rates. Average MAC delay is the sum of two components - the channel access time, and the average waiting time in a BI. The stations that fail to transmit an ATIM frame successfully in the ATIM window, have to wait for the rest of the BI to get next chance in the next ATIM window. This increases the average waiting time to get a chance to transmit data frames. For this reason, average delay increases with the increase of BI size. Fig. 8 shows the impact of the network size over the MAC delay for different data arrival rates. When data arrival rate is low and the network is unsaturated, the end to end MAC delay does not differ too much for different network sizes. For higher data arrival rates, the MAC delay increases as the network size increases. Further, increasing the data arrival rate also prolongs the MAC delay. Therefore, the MAC delay mainly depends on the network contention. During network unsaturation, network size has comparatively lower impact over the channel contention, and so, the MAC delay does not get affected. In network saturation, the contention among stations increases as the network size increases. The channel contention increases even further, as the data arrival rate increases. Thus the MAC delay rises significantly with the network size and the data arrival rate.

Fig. 9 shows the average power consumption with respect to the data arrival rate. The result obtained from the analytical model for power consumption in section 5 has been verified through simulation. Fig. 9 shows that the simulation result matches with the theoretical analysis. The impact of the network size and the BI size on the power consumption is presented in Fig. 10 and Fig. 11. Fig. 10 gives a comparison of average power consumption for different BI (for fixed ATIM window) against the data arrival rate. It is clear from the figure that as the size of the BI increases, the average power consumption decreases. A station that neither transmits

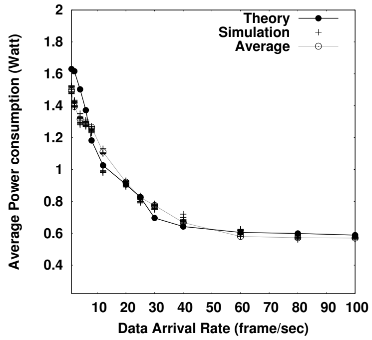

Fig. 9. Power for $n = 20$

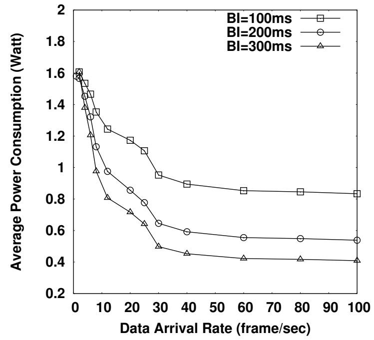

Fig. 10. Power for $n = 20$

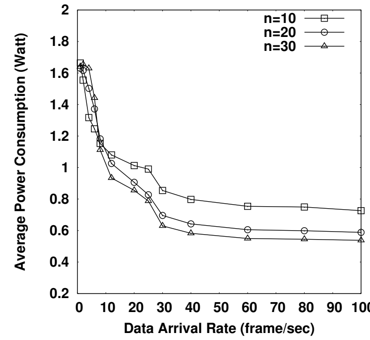

Fig. 11. Power for $BI = 200$

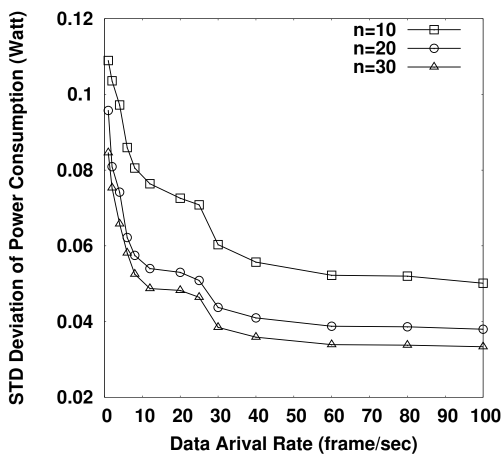

Fig. 12. Standard Deviation of Power Consumption

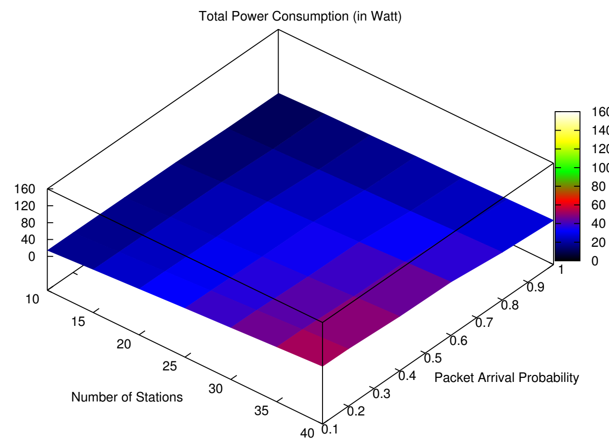

Fig. 13. Total Power Consumption in PSM

an ATIM frame successfully nor receives an ATIM frame remains in sleep mode for a long time when the BI is large. It is also observed that as the data arrival rate increases, the amount of power consumption decreases. A higher data arrival rate implies more number of stations contending at the ATIM window for successfully transmitting ATIM frames. This increased contention reduces the percentage of stations that get a chance to participate in the data communication. The remaining stations go to sleep mode in the data window. Thus the average power consumption decreases. During unsaturation, the average power consumption decreases slowly and then becomes constant at the network saturation state. Fig. 11 presents the average power consumption for different network sizes. It is clear from the figure that the average power consumption for a network of size 10 is more than the average power consumption for a network of size 20. This is because contention is less for a small network, and so, most of the stations are in transmit or receive state, leading to higher power consumption. Fig. 9 to Fig. 11 show that IEEE 802.11 PSM saves significant amount of power by letting stations go to sleep when there is no data to transmit or receive. However, to improve network lifetime through power saving, power consumption should be uniform throughout the network. For example, if a station consumes more power compared to other stations, it may soon die-out resulting in a negative impact over network lifetime. The distribution of power saving throughout the network can be analyzed by computing standard deviation of power consumption among all the stations in the network. The standard deviation of the power distribution among the stations is shown in Fig. 12, as derived from the theoretical model presented in this paper. It can be seen from the figure that the value of the standard deviation is very low. The deviation of power among the stations is less than 10%. This indicates that the power consumption is uniformly distributed among all the stations in the network. Hence, no station in the network dissipates considerably high power compared to others, which in turn increases the network lifetime.

Fig. 13 to Fig. 16 give a comparative study of the power consumption between IEEE 802.11 with and without power save mode. The results for IEEE 802.11 DCF without PSM analysis is obtained from simulation with similar parameters as shown in Table 1. The packet availability probability is calculated from the traffic generation rate according to equation (18). Fig. 13 shows the total power consumption in IEEE 802.11 PSM with respect to the number of stations and the packet availability probability. Fig. 14 shows the same for IEEE 802.11 running without PSM enabled. These two figures

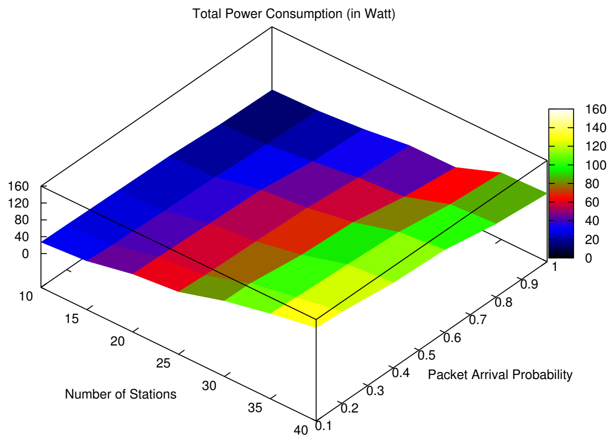

Fig. 14. Total Power Consumption without PSM

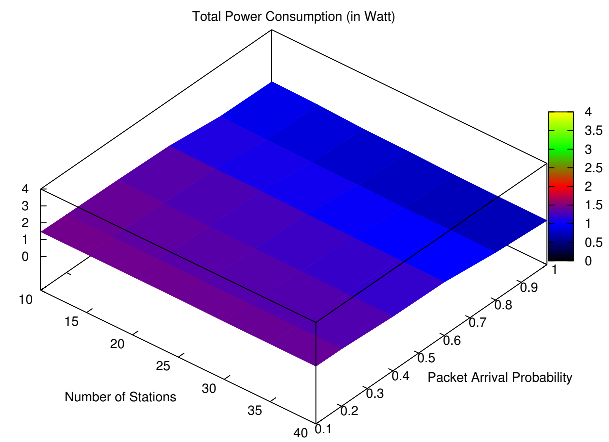

Fig. 15. Average Power Consumption in PSM

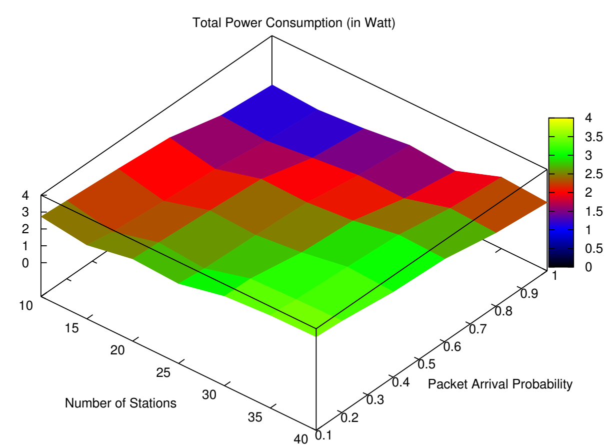

Fig. 16. Average Power Consumption without PSM

clearly indicate that total power consumption in PSM is significantly less compared to IEEE 802.11 without PSM. Further in PSM (as well as without PSM) total power consumption increases as the packet availability probability decreases. This is because in PSM a station needs to remain in the power on mode if it successfully transmits an ATIM frame in the ATIM window. Therefore at a low data rate, even if the station does not have data to transmit, it needs to remain in the power on mode in the entire data window, after transmitting the data from its interface buffer. Fig. 15 and Fig. 16 show the comparison of average power consumption per station in PSM and without PSM. It can be seen from the figures, that as the number of station increases, the average power consumption decreases in PSM, whereas, the average power consumption increases in without PSM. In PSM, the stations that do not have any data to transmit go to sleep to save power. Thus with a large number of stations, the stations that cannot transmit or receive an ATIM frame successfully, go to sleep. This reduces average power consumption with a large number of nodes. Again with a higher data rate, contention among stations increases, and thus the stations that fail to transmit or receive an ATIM frame, go to sleep. This further reduces average power consumption.

The observations from the above analysis can be summarized as follows:

1) As the BI increases, the network throughput increases and the average power consumption decreases. However the average MAC delay increases because of the large waiting time. Thus for a delay tolerant network, a larger BI can give an effective network performance. However, for delay sensitive applications, BI should be chosen based on the application requirement. A dynamic and adaptive BI can provide better performance based on application sensitivity.
2) As the number of stations increases, the network throughput decreases and the MAC delay increases. One important observation is that the average power consumption also decreases with the increase in network size, as the power saving is uniform throughout the network.
3) The PSM of IEEE 802.11 DCF saves substantial amount of battery power. When a node does not have data to transmit, or it does not receive any data from other nodes, the node goes to sleep. Further at high contention, the nodes that fail to transmit or receive ATIM frames, also go to sleep. This reduces the average power consumption as well as contention in the data window.

7 Conclusion

This paper proposes an analytical model for IEEE 802.11 IBSS PSM at different traffic conditions. The data frame transmission along with the corresponding ATIM frame transmission is modeled using a discrete time Markov chain. The network performance parameters, such as overall normalized throughput, average MAC delay and average power consumption is calculated from the Markov chain model. The analysis shows that there is a trade-off among throughput, MAC delay and average power consumption. A dynamic and adaptive BI can provide better power saving with little compromise in delay and throughput, that can open several directions for future research.

References

[1] *IEEE Std 802.11-2007, Part 11: Wireless LAN Medium Access Control (MAC) and Physical Layer (PHY) Specifications, Edition 2007*, IEEE.

[2] M. Ergen and P. Varaiya, "Decomposition of energy consumption in IEEE 802.11," in *Proceedings of IEEE International Conference on Communications*, 2007.

[3] G.Bianchi, "Performance analysis of the IEEE 802.11 distributed coordination function," *IEEE Journal on Selected Areas in Communications*, vol. 18, no. 3, pp. 535–547, March 2000.

[4] A. Alshanyour and A. Agarwal, "Three-dimensional markov chain model for performance analysis of the IEEE 802.11 distributed coordination function," in *Proceedings of the 28th IEEE conference on Global telecommunications*, 2009, pp. 2510–2516.

[5] H. Wo, Y. Peng, K. Long, S. Cheng, and J. Ma, "Performance of reliable transport protocol over IEEE 802.11 wireless LAN: Analysis and enhancement," in *Proceedings of Annual Joint Conference of the IEEE Computer and Communications Societies*, 2002.

[6] R. Wang, J. Zhang, and X. Zou, "Performance analysis and optimization of IEEE 802.11 DCF with constant contention window," in *Proceedings of IEEE International Conference on Electronics, Circuits, and Systems*, Aug 2008.

[7] Y. Xiao, "Performance analysis of priority schemes for IEEE 802.11 and IEEE 802.11e wireless LANs," *IEEE Transactions on Wireless Communications*, vol. 4, no. 4, pp. 1506–1515, 2005.

[8] A. Balachandran, G. M. Voelker, P. Bahl, and P. V. Rangan, "Characterizing user behavior and network performance in a public wireless LAN," *SIGMETRICS Performance Evaluation Review*, vol. 30, no. 1, pp. 195–205, Jun. 2002.

[9] "Qualnet 5.0.1 Network Simulator, http://www.scalable-networks.com/products/qualnet/."

[10] M. Ergen and P. Varaiya, "Throughput analysis and admission control for IEEE 802.11a," *Journal of Mobile Networks and Applications*, vol. 10, no. 5, pp. 705–716, 2005.

[11] Y. Zheng, K. lu, D. Wu, and Y. Fang, "Performance Analysis of IEEE 802.11 DCF in Imperfect Channels," *IEEE Transaction on Vehicular Technology*, vol. 55, pp. 1648–1656, Sep. 2006.

[12] D. Malone, K. Duffy, and D. Leith, "Modeling the 802.11 DCF in Nonsaturated Heterogeneous Condition," *IEEE Transaction on Networking*, vol. 15, pp. 159–172, Feb. 2007.

[13] F. Daneshgaran, M. Laddomada, and M. Mondin, "Unsaturated Throughput Analysis of IEEE 802.11 DCF in the Presence of Non Ideal Transmission Channel and Capture Effects," *IEEE Transaction on wireless communications*, vol. 7, pp. 1276–1286, APRIL 2008.

[14] F. Yi and I. Marsic, "Analysis of Non-saturated and Saturated Performance of IEEE 802.11 DCF in the Presence of Hidden Stations," in *Proceedings of IEEE Vehicular Technology Conference*, 2007.

[15] L. M. Feeney and M. Nilsson, "Investigating the energy consumption of a wireless network interface in an ad hoc networking environment," in *Proceedings of Annual Joint Conference of the IEEE Computer and Communications Societies*, 2001, pp. 1548–1557.

[16] I. Ramachandran, A. K. Das, and S. Roy, "Analysis of the contention access period of IEEE 802.15.4 MAC," *ACM Transaction on Sensor Networks*, vol. 3, no. 1, Mar. 2007.

[17] A. Garcia-Saavedra, P. Serrano, A. Banchs, and G. Bianchi, "Energy consumption anatomy of 802.11 devices and its implication on modeling and design," in *Proceedings of the 8th international conference on Emerging networking experiments and technologies*. ACM, 2012, pp. 169–180.

[18] P. Swain, S. Chakraborty, S. Nandi, and P. Bhaduri, "Performance modeling and evaluation of IEEE 802.11 IBSS power save mode," *Ad Hoc Networks*, vol. 13, Part B, pp. 336 – 350, 2014.

[19] E. S. Jung and N. H. Vaidya, "Energy efficient MAC protocol for wireless LANs," in *Proceedings of Annual Joint Conference of the IEEE Computer and Communications Societies*, 2002.

[20] R. Zheng, J. C. Hou, and L.Sha, "Performance analysis of the IEEE 802.11 power save mode," in *Proceedings of IEEE International Symposium of Computer Networks and Distributed Systems*, January 2004.

[21] M. Cao, W. Ma, Q. Zhang, X. Wang, and W. Zhu, "Modelling and performance analysis of the distributed scheduler in IEEE 802.16 mesh mode," in *Proceedings of the 6th ACM international symposium on Mobile ad hoc networking and computing*, 2005, pp. 78–89.

[22] S. M. Ross, *Introduction to Probability Models*, 10th ed. Academic Press, 2009.

[23] "Cisco Aironet 350 Series Client Adapters, http://www.cisco.com/en/US/prod/collateral/wireless/ps6442/ps4555/ps448/product_data_sheet09186a0080088828.html."

Pravati Swain Pravati Swain received her PhD degree from the Indian Institute of Technology, Guwahati, India. At present, she is a postdoctoral research fellow at University of Missouri, Kansas City. Her research interests include performance modeling and analysis of computer networks. Dr. Swain is a student member of IEEE and Association for Computing Machinery (ACM).

Sandip Chakraborty Sandip Chakraborty received his PhD degree from the Indian Institute of Technology Guwahati, India. At present, he is an Assistant Professor at the Indian Institute of Information Technology, Guwahati. His research interests include wireless networks and mobile computing. Dr. Chakraborty is a Student Member of IEEE, IEEE Communications Society, ACM and ACM SIGCOMM.

Sukumar Nandi Sukumar Nandi received the PhD degree from the Indian Institute of Technology Kharagpur, India. He is currently a Professor of Computer Science and Engineering with Indian Institute of Technology, Guwahati, India. His research interests include wireless networks, network security and distributed computing. Dr. Nandi is a Senior Member of IEEE, a Senior Member of ACM, a Fellow of The IE(India) and a Fellow of The IETE(India).

Purandar Bhaduri Purandar Bhaduri received the Ph.D. degree from the Washington State University, Pullman in 1993. Presently he is working as a Professor at the Department of Computer Science and Engineering at the Indian Institute of Technology Guwahati, India. His current research interests include formal modeling and verification of embedded control systems and formal foundations for component-based embedded control systems.